New Journal of Physics
The open access journal at the forefront of physics

Deutsche Physikalische Gesellschaft DPG IOP Institute of Physics

PAPER • OPEN ACCESS

Multilayer coevolution dynamics of the nonlinear voter model

To cite this article: Byungjoon Min and Maxi San Miguel 2019 *New J. Phys.* **21** 035004

IOP Publishing New J. Phys. 21 (2019) 035004 https://doi.org/10.1088/1367-2630/ab0985

New Journal of Physics
The open access journal at the forefront of physics

Deutsche Physikalische Gesellschaft DPG
IOP Institute of Physics

Published in partnership with: Deutsche Physikalische Gesellschaft and the Institute of Physics

CrossMark

OPEN ACCESS

RECEIVED
29 November 2018

REVISED
7 February 2019

ACCEPTED FOR PUBLICATION
22 February 2019

PUBLISHED
19 March 2019

PAPER

Multilayer coevolution dynamics of the nonlinear voter model

Byungjoon Min[1,2] and Maxi San Miguel[1]

[1] IFISC, Instituto de Física Interdisciplinar y Sistemas Complejos (CSIC-UIB), Campus Universitat de les Illes Balears, E-07122 Palma de Mallorca, Spain
[2] Department of Physics, Chungbuk National University, Cheongju, Chungbuk 28644, Republic of Korea

E-mail: maxi@ifisc.uib-csic.es

Keywords: coevolutionary dynamics, multilayer networks, nonlinear voter model

Abstract

We study a coevolving nonlinear voter model (CNVM) on a two-layer network. Coevolution stands for coupled dynamics of the state of the nodes and of the topology of the network in each layer. The plasticity parameter p measures the relative time scale of the evolution of the states of the nodes and the evolution of the network by link rewiring. Nonlinearity of the interactions is taken into account through a parameter q that describes the nonlinear effect of local majorities being $q = 1$ the marginal situation of the ordinary voter model. Finally the connection between the two layers is measured by a degree of multiplexing ℓ. In terms of these three parameters, p, q and ℓ we find a rich phase diagram with different phases and transitions. When the two layers have the same plasticity p, the fragmentation transition observed in a single layer is shifted to larger values of p plasticity, so that multiplexing avoids fragmentation. Different plasticities for the two layers lead to new phases that do not exist in a CNVM in a single layer, namely an asymmetric fragmented phase for $q > 1$ and an active shattered phase for $q < 1$. Coupling layers with different types of nonlinearity, $q_1 < 1$ and $q_2 > 1$, we can find two different transitions by increasing the plasticity parameter, a first absorbing transition with no fragmentation and a subsequent fragmentation transition.

1. Introduction

Real-world networked systems ranging from biological systems [1, 2] and human society [3, 4] to transportation [5] and infrastructure systems [6–8] are rarely isolated but often formed by multiple layers of networks. In order to perform functionality properly, the networked systems maintain multilayer structures and interactions between different layers of networks. The concept of multilayer networks [9] has been proposed along with interconnected networks [10], interdependent networks [11], and multiplex networks [12], for a more complete modeling of interconnected systems. Multilayer networks are a framework not only for a better description of complex systems but also for novel dynamical processes that cannot be captured in a single layer framework [9, 13–15]. Indeed, several studies on multilayer networks show that interlayer connections account for significant differences in many phenomena, including percolation [10, 16, 17], diffusion [18], epidemic spreading [19–22], cascade of failures [11, 23], opinion formation [15, 24–26], online communities [27], game theory [28–30] or cultural dynamics [31].

One fundamental feature studied in multilayer networks is coevolution dynamics [24, 27, 32], that is the evolution of a network structure in response to the dynamical processes that change the state of the nodes [33]. A coevolving voter model is a representative model of coevolution dynamics on complex networks [34, 35]. An ordinary coevolving voter model consists of two different kinds of processes: copying and rewiring. The ratio of time scales at which these two processes occur is measured by a parameter p called plasticity of the network. For the copying process, with a certain probability p a node changes its state by copying the state of one of its neighbors randomly chosen, following the original imitation mechanism implemented by the voter model. For the rewiring process, with the complementary probability $1-p$ a node rewires its connection with a neighbor having a different state, to another node having the same state. The ordinary coevolving voter model exhibits an absorbing phase transition between an dynamically active coexistence phase and an absorbing phase in the thermodynamic limit [34]. The finite size manifestation of this transition is a network fragmentation transition. Coevolution dynamics of the voter model on multilayer networks gives a more complete modeling of real world situations: for instance, the individuals' opinion and social networks may evolve through multiple different types of social relationship, such as family, friends, and colleagues, or communication, friendship and trade networks. An important parameter in this multilayer description is the degree of multiplexity measured by the density of interlayer links, i.e. density of links between nodes in different layers. It has been found that a coevolving voter model in a multilayer network exhibits a shattered fragmentation with a phase showing many disjointed small components [24]. This phase does not exist in a coevolving voter model in a single network layer. In addition, it has also been shown that the voter model on multilayer networks cannot be reduced to a single layer description [15]. Therefore, the structure of multilayer networks significantly affects the dynamical consequences of coevolution in the voter model [24, 27].

More recently, collective or group interactions beyond the dyadic interactions of the voter model have been considered within a coevolution dynamics context [36, 37]. Specifically, a coevolving nonlinear voter model (CNVM) has been studied in order to incorporate collective interactions and coevolution dynamics at the same time [36]. The nonlinearity in the CNVM takes into account that the state of an agent is affected by the state of all of their neighbors as a whole, and not by a pairwise interaction [38–41]. The nonlinear interaction gives rise to diverse phases, with different mechanisms for fragmentation transitions. Such form of nonlinearity was also studied in social impact theory [42], in language evolution problems [43], or in language competition dynamics under the name of volatility [44–46]. However, the effect of the nonlinearity in a coevolving voter model has been examined only on a single layer network as the simplest example.

In view of the nontrivial modifications found for a coevolving voter model when considering a multilayer framework, we address in this paper the study of a CNVM on a multilayer network. The outline of the paper is as follows. In section 2 we specify our dynamical model. Section 3 describes our results for the case in which the two layers have the same plasticity p. In this case we find that the fragmentation transition found in a single layer [36] continues to exist, but with a delayed threshold of p. Our numerical results are qualitatively described by a mean-field approach. Section 4 considers the case in which the two layers have different plasticities, and we find a rich variety of phases such as a dynamically active shattered phase, an asymmetric fragmented phase, and a coexistence phase. In section 5 we analyze the case of layers with different nonlinearity which also results in other non-trivial phase transitions that are not observed in a single layer network. For instance, two subsequent transitions can occur among coexistence, consensus, and absorbing fragmented phases.

2. Model

Our model considers multilayer networks composed of two different layers in which each layer is initially independently constructed as a degree regular network with the same number of nodes N and with the same number $\langle k \rangle = 4$ of random intralayer links for each node. Inter-layer links connect two nodes that belong to the two different layers (figure 1). We define the degree of multiplexity ℓ [24] as the density of inter-layer links so that ℓN is the total number of links connecting nodes in different layers. Initially each node i is in one of two states, $s_i = +1$ (up) or -1 (down), with the same probability $1/2$, and it has the same state in both layers. At a given configuration, links between two nodes in the same layer (intra-links) can be classified as active or inert, depending on the state of the pair of connected nodes. Active (inert) links stand for the links connecting two nodes in different (same) states.

The dynamical model is as follows: at each step, we randomly choose a layer and a node i in the chosen layer. We measure the fraction of active links of node i with respect to its degree k_i, $\left(\frac{a_i}{k_i}\right)$ where a_i is the number of active links of node i. Nonlinear interactions are implemented through a probability $\left(\frac{a_i}{k_i}\right)^q$, where q is the nonlinearity parameter measuring the nonlinear effect of local majorities in the selection on pair interacting agents. With this probability, the node i takes an action of either copying or rewiring. Then, we choose one of its neighbors j, having a state different than the one of node i (or equivalently we choose one of the active links of node i). Note that with the complementary probability $1 - \left(\frac{a_i}{k_i}\right)^q$, nothing happens and another node is randomly selected. Next, rewiring occurs with probability p: the chosen active link is removed, and rewired to a new node having the same state as the state of node i. And, with probability $1-p$ node i changes its state by copying the state of node j. Subsequently, a node connected to i in the other layer by an inter-link also changes its state adopting the same state than node i. This synchronization process leads to the same state for connected nodes across different layers. While the number of nodes and the density of links are constant, the network structure and the configuration of the states of the state vary in time. These update processes proceed until the system reaches a steady state.

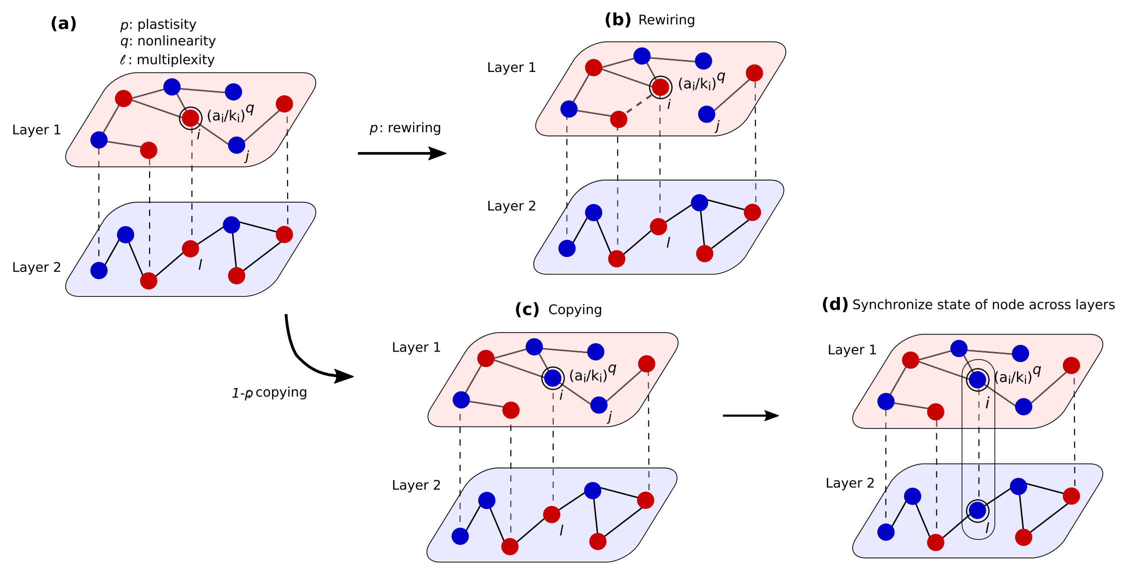

Figure 1. Schematic illustration of update rules in a nonlinear coevolving voter model on multilayer networks. At each step, a layer and node i in the layer are chosen randomly. Then, with a probability $\left(\frac{a_i}{k_i}\right)^q$ one of the active links is chosen. And, we rewire an active link with probability p and copy the state of the chosen neighbor with probability $1-p$. If node i is connected to a node in the other layer, the state of the node in the other layer is synchronized to its state with the state of i.

In our model, we have three main parameters: plasticity or rewiring rate p, nonlinearity q, and the degree of multiplexity ℓ. First, the plasticity measures how often the process of rewiring occurs as compared to the process of copying. When $p = 0$, a network is static, so that the model becomes the voter model on multilayer networks [15]. On the other hand, when p is non-zero, both the structure of the network and the state of the nodes in the network change in a coevolution dynamics. In the other extreme $p = 1$, there is no copying process and the network eventually becomes fragmented due to the rewiring processes. Second, the nonlinearity parameter q measures the effect of local group interactions. Nonlinearity is mathematically implemented as $\left(\frac{a_i}{k_i}\right)^q$ [36, 38–41]. When $q = 1$, our model becomes the ordinary coevolving linear voter model [34]. For $q > 1$, nodes with more active links have a higher probability, as compared to the ordinary linear voter model, to take an action than other nodes. When $q < 1$, nodes with less active links are more likely to take action than in the linear voter model. Finally, the degree of multiplexity ℓ stands for the density of interlayer links. $\ell = 1$ corresponds to one-to-one connections among the nodes in the two layers, while $\ell = 0$ corresponds to the case of no interconnections, meaning that the two layers are isolated. When $0 < \ell < 1$, the networks on the two layers are interconnected but have sparse interconnections than one-to-one connections.

3. Symmetric plasticity in multilayer networks

We indicate as p_1 and p_2 the plasticities of each layer. The simplest case of the coevolving model on multilayer networks is the case of symmetric plasticity, so that $p = p_1 = p_2$. To describe the properties of the steady state, we use the size S of the largest network component for measuring the global connectivity and the absolute value $|m|$ of magnetization $m = \sum_i s_i$ for each layer. For a single layer, the nonlinearity q significantly changes the coevolution dynamics [36]: when $q < 1$, a fragmentation transition between a dynamically active coexistence phase in a single component network and a fragmented phase occurs for a critical plasticity p_c, while when $q > 1$ a distinct type of a fragmentation transition occurs between an absorbing consensus phase and a fragmented phase. When $q = 1$, which is the case of the ordinary linear voter model, an absorbing phase transition between a dynamically active coexistence phase and an absorbing phase in a fragmented network is recovered [34, 36]. Note that in the long time limit the active phase for the linear case $q = 1$ can survive only for the thermodynamic limit $N \to \infty$ since for any finite systems the active phase falls into a consensus phase due to finite size fluctuations [34, 36].

The same phases and transitions described for the single layer case continue to exist in multi-layer networks but the critical plasticity p_c is delayed as the degree of multiplexity ℓ increases. For different nonlinearity parameters $q = 0.5$, 1, and 2, we determine S, $|m|$, and the characteristic time τ to reach a final state (figure 2). Note that S, $|m|$, and τ for both layers are statistically the same due to the symmetric case analyzed here. When $q = 0.5$, we find an absorbing phase transition between a coexistence phase and a fragmented phase. This

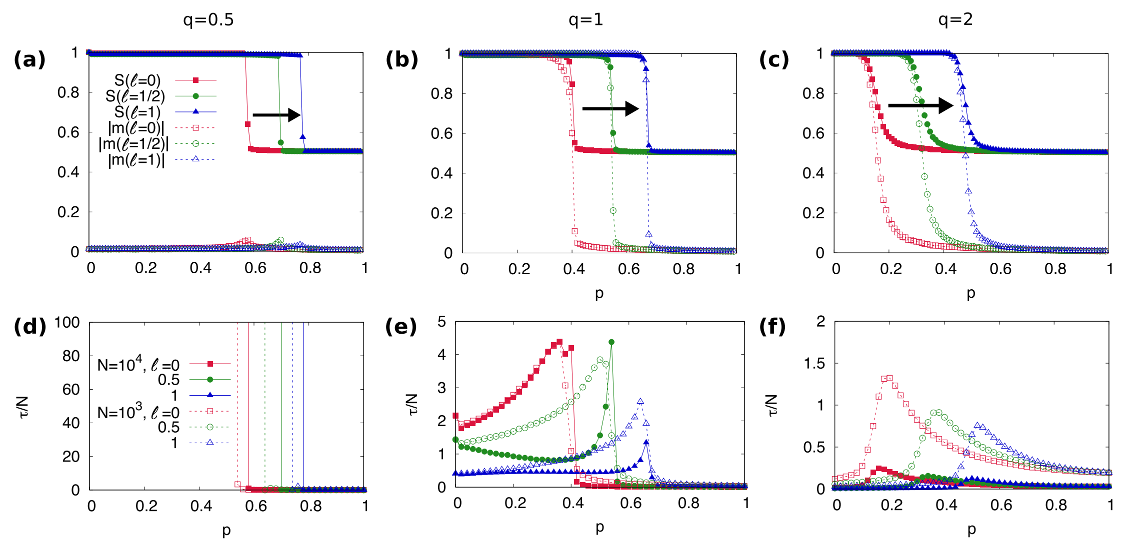

Figure 2. The size S of the largest component and the absolute value $|m|$ of magnetization of (a) $q = 0.5$, (b) 1, and (c) 2 with symmetric plasticity $p = p_1 = p_2$ for different $\ell = 0, 0.5, 1$ on multilayer degree regular networks with $\langle k \rangle = 4$ and $N = 10^4$ for each layer, averaged over 10^4 runs. The characteristics time τ to reach the final state of (d) $q = 0.5$, (e) 1, and (f) 2 is also shown for $N = 10^3$ and 10^4.

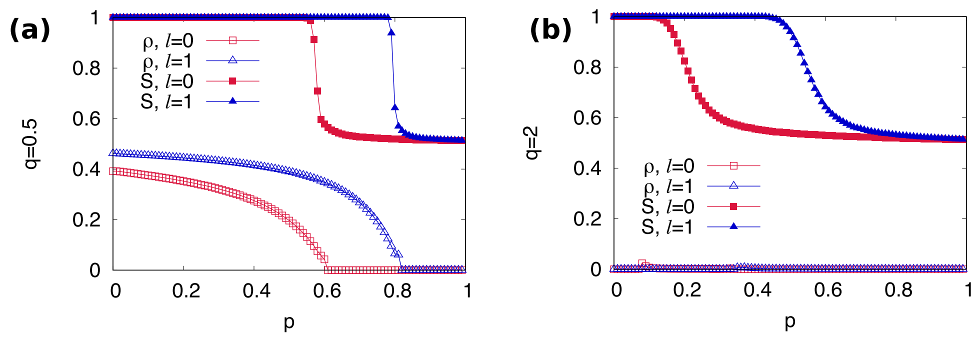

Figure 3. The density ρ of active links and the size S of the largest component with symmetric plasticity $p = p_1 = p_2$ for different $\ell = 0,1$ with $\langle k \rangle = 4$ and $N = 10^3$ for each layer.

absorbing phase transition is clearly identified by looking at the density ρ of active links in either of the two equivalent layers (figure 3). The coexistence phase, which is dynamically active, is well characterized by a finite value of ρ and by the divergence of τ in the thermodynamic limit $N \to \infty$. The fragmented phase corresponds to $\rho = 0, S = 1/2$ and $m = 0$, implying two disjoint clusters, each of them in a consensus state but but with opposite consensus states. When $q = 2$, we find a different transition at the critical plasticity p_c between two absorbing phases, a consensus and a fragmented phase. The consensus phase is characterized by $\rho = 0, S = 1$ and $|m| = 1$, implying a single network component with an ordered state. Therefore, we can conclude that the fragmentation transition for $q = 0.5$ and $q = 2$ is qualitatively different. For $q = 0.5$, we find a continuous absorbing phase transition, characterized by the density of active links ρ. But, for $q = 2$, we find a different transition between two absorbing phases, a consensus and a fragmented phase. More details on the nature of these transitions were discussed elsewhere [36]. For the linear case $q = 1$ [24], we also observe a delay of the fragmentation transition when increasing the degree of multiplexity. We have checked that the delay of the transition is a robust feature for networks with different average degree $\langle k \rangle = 8,\ 16$, as shown in figure 4(a), (b). We also find that the transition point p_c becomes larger as $\langle k \rangle$ increases. In addition, we find that the fragmentation transition and the shift of p_c as p increases persists for considerably large values of q, i.e. $q = 4, 8, 16$ (figure 4(c)).

We further examine the effect of the multiplexity in terms of the dependence p_c on ℓ for $q = 0.5$ and 2 (figure 5). For both $q = 0.5$ and 2, we find a delayed onset (larger p_c) of the fragmented phase with increasing multiplexity ℓ. The shift of p_c means that the inter-layer connections in a multilayer structure prolong the global connectivity in the coevolution dynamics: multiplexity provides a source of disorder due to the synchronization process. Therefore increasing the degree of multiplexity ℓ leads to the shift of p_c. This the same mechanism that

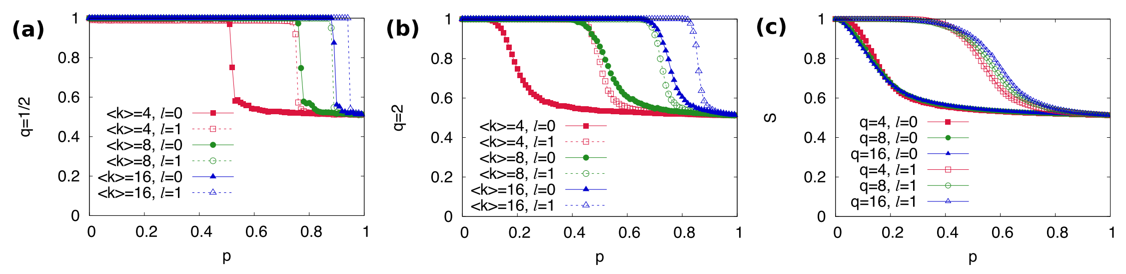

Figure 4. The size of the largest cluster for (a) $q = 1/2$ and (b) $q = 2$ with different $\langle k \rangle = 4,\ 8,\ 16$. (c) The size of the largest cluster for large $q = 4, 8, 16$ for with $\ell = 0$ and $\ell = 1$.

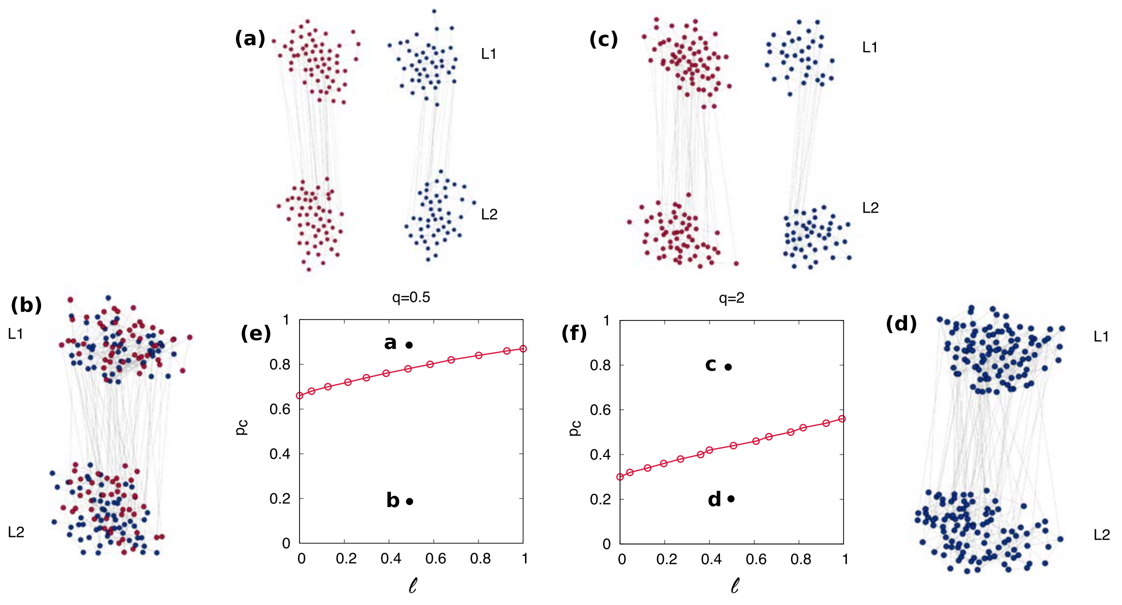

Figure 5. Phase diagram for the symmetric plasticity case with (e) $q = 0.5$ and (f) $q = 2$ together with network examples of (a) fragmented $(p, q, \ell) = (0.9, 0.5, 0.5)$, (b) coexistence $(0.2, 0.5, 0.5)$, (c) fragmented $(0.8, 2, 0.5)$, and (d) consensus $(0.2, 2, 0.5)$ phases. The phase diagram is obtained numerically with initial multilayer degree regular networks with $\langle k \rangle = 4$ and $N = 10^3$. The lines in the diagram are just to guide the eyes.

for the linear voter model and therefore both for linear and nonlinear interactions, multiplexity prevents fragmentation. However, the role of nonlinearity is shown in the final state: a dynamically active coexistence phase in $q = 0.5$ and a consensus phase in $q = 2$.

In order to obtain an analytic insight for the shift of p_c, we introduce mean-field equations [24, 34, 36, 40] for the nonlinear voter model on multilayer networks. These equations are valid in the thermodynamic limit $N \to \infty$. We define the average degree of each layer as $\langle k_1 \rangle$ and $\langle k_2 \rangle$. The density of active links ρ_i in each layer $i \in \{1,\ 2\}$ can be described by the following equations [36, 40]

$$\frac{\mathrm{d}\rho_i}{\mathrm{d}t} = -\rho_i^q p_i + \rho_i^q (1 - p_i)[\langle k_i \rangle - 2q - 2(\langle k_i \rangle - q)\rho_i] + \ell \rho_j^q (1 - 2\rho_i)\langle k_i \rangle. \tag{1}$$

Note that these coupled equations reduce to previous results in the appropriate limit of linear interactions $q = 1$ [24] or decoupled layers $\ell = 0$ [36]. Assuming that the two layers have the same mean degree $(\langle k \rangle = \langle k_1 \rangle = \langle k_2 \rangle)$, and for symmetric coupling $(p = p_1 = p_2)$

$$\frac{\mathrm{d}\rho}{\mathrm{d}t} = -\rho^q p + \rho^q (1 - p)[\langle k \rangle - 2q - 2(\langle k \rangle - q)\rho] + \ell \rho^q (1 - 2\rho)\langle k \rangle, \tag{2}$$

where $\rho = \rho_1 = \rho_2$ due to the symmetry. For the steady state, the trivial solution $\rho = 0$ corresponds to a fragmentation state where the dynamics is frozen and the non-zero solution corresponds to a dynamically active state. The non-zero solution ρ^* of equation (2) gives

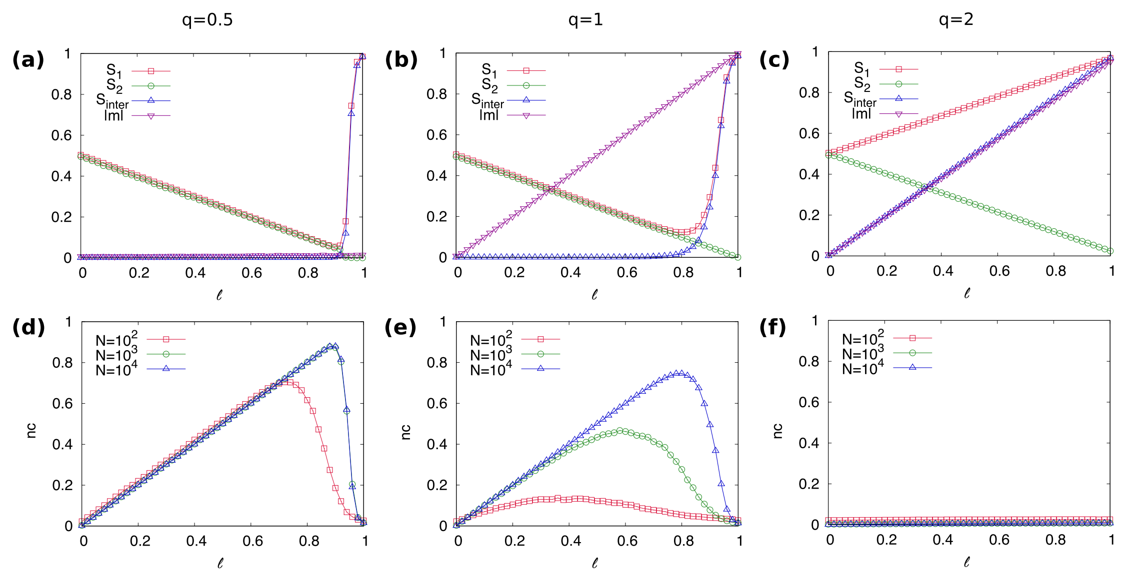

Figure 6. For a bilayer with fully asymmetric plasticity $p_1 = 1$ and $p_2 = 0$ the following quantities for the dynamic layer $p_1 = 1$ are shown: size S_1 of the largest component, size S_2 of the second largest component, the fraction S_{inter} of nodes having interconnections in the largest network component and the absolute value $|m|$ of magnetization for (a) $q = 0.5$, (b) 1, and (c) 2. Numerical simulations on multilayer initially degree regular networks with $\langle k \rangle = 4$ and $N = 10^4$ for each layer. The relative number of network components nc of the dynamic layer for (d) $q = 0.5$, (d) 1, and (f) 2 is also reported for different system sizes.

$$\rho^* = \frac{\langle k \rangle (1 + \ell - p) - 2q + p(2q - 1)}{2\langle k \rangle (1 + \ell - p) + (1 - p)q}. \tag{3}$$

The transition point to the fragmentation phase with $\rho = 0$ is

$$p_c = \frac{\langle k \rangle + \ell \langle k \rangle - 2q}{1 + \langle k \rangle - 2q}. \tag{4}$$

Thus, this mean-field approximation accounts for the linear growth of p_c with respect to ℓ obtained numerically. The analytical approach predicts successfully the shift of p_c but it gives quantitatively inaccurate values of p_c as it is also the case for the linear voter model [24]. The mean-field approximation predicts that the transition appears in a narrow range of parameter values for $\langle k \rangle$ and q. However, our numerical simulations discussed above (figure 4) show that the transition is robust against changes of these parameters.

4. Asymmetric plasticity in multilayer networks

Far from the symmetric case, an extreme coupling scenario is that of fully asymmetric plasticity, meaning that one layer only rewires ($p_1 = 1$, the dynamic layer) and the other layer only changes the state of the nodes ($p_2 = 0$, the voter layer). The dynamic layer is affected by the voter layer due to the synchronization step, but the voter layer is independent of the dynamic layer. Hence as $t \to \infty$, the voter layer will either remain in an active coexistence phase ($q < 1$), except for finite size effects, or will reach a consensus phase ($q > 1$), as the result of the single layer dynamics [36]. However, the dynamic layer can show a variety of asymptotic states depending on the nonlinearity q and the degree of multiplexity ℓ. It is worthwhile to mention that we use the random rewiring when finding a new connection in a dynamic layer. But, different rewiring protocols such as rewiring based on the principle eigenvalue of adjacency matrix [47, 48], local rewiring [37], and preferential attachment rewiring [49] may bring out different phenomena such as localization of multilayer networks [47]. In order to describe these possible states, we determine in the dynamic layer, and for $q = 0.5, 1, 2$, the size of the largest network component S_1, the size of the second largest network component S_2, the absolute value $|m|$ of magnetization, and the relative number of components nc to the network size N, as shown in figure 6. In addition, we also determine the fraction S_{inter} of nodes in the dynamic layer that belong to the largest network component S_1 and at the same time are connected to the voter layer. Since in our model only a fraction of nodes (ℓN) have interlayer links, S_{inter} refers to the fraction of nodes of the largest network component with interlayer links. Note that $S_{\text{inter}} \leqslant S_1$ and $S_{\text{inter}} \leqslant \ell N$.

When $q = 1$ (the linear voter case [24]), we find a shattered phase in the dynamic layer for a broad range of values of ℓ, showing two large components in opposite states and many isolated nodes (figures 6(b), (e)). This

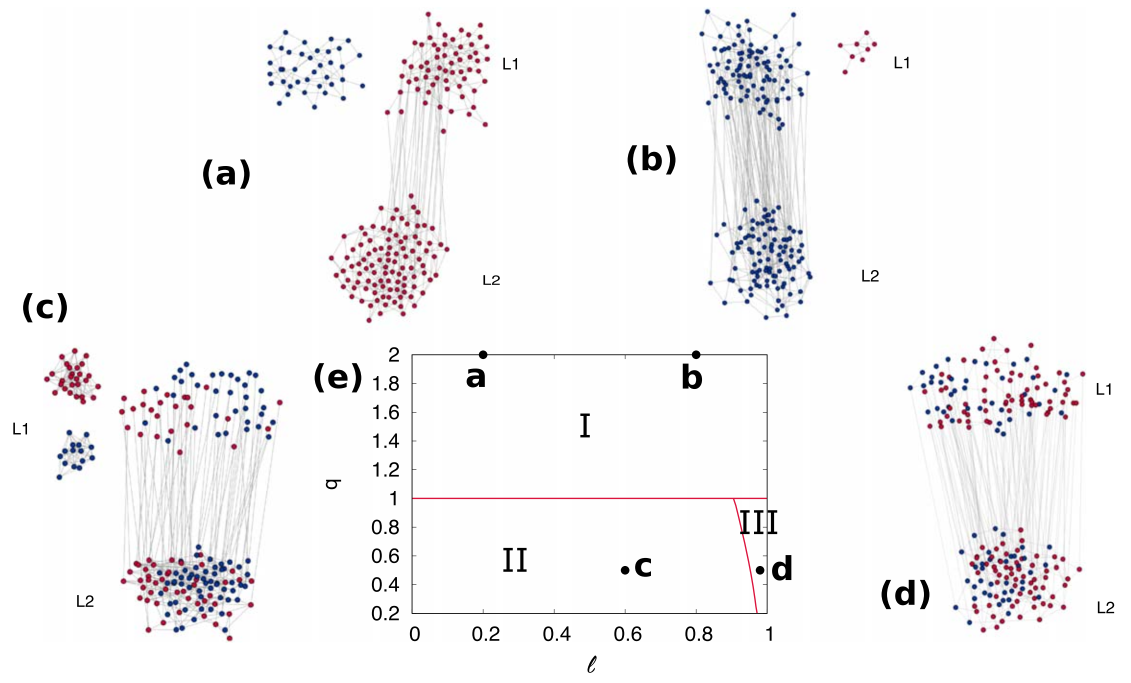

Figure 7. Phase diagram (e) for the fully asymmetric plasticity case ($p_1 = 1$ and $p_2 = 0$). Network configuration of (a) asymmetric fragmented phase $(q, \ell) = (2, 0.2)$, and (b) $(2, 0.8)$, (c) shattered phase $(0.5, 0.6)$, and (d) coexistence phase $(0.5, 0.95)$. The phase diagram is obtained numerically with multilayer initially degree regular networks with $\langle k \rangle = 4$ and $N = 10^3$.

shattered phase appears because nodes in the voter layer drive the separation of nodes in the dynamic layer by the synchronization step of the dynamics.

When $q = 0.5$, a representative example of $q < 1$, the structure of the dynamical layer evolves to a shattered phase where two significant network components are in opposite states and many small clusters exist for a wide range of ℓ similarly to the linear voter case ($q = 1$). The relative number of components nc clearly identifies the existence of many isolated nodes in the dynamic layer (figure 6(d)). As ℓ increases from zero, nc increases linearly and S_1 and S_2 decreases linearly as well. S_{inter} is nearly zero for all ℓ, indicating that the nodes having interlayer links are those which are isolated in their layer. However, the absolute value of the magnetization $|m|$ in the dynamical layer remains zero at variance with what happens for $q = 1$. This neutral magnetization is caused by a dynamically active coexistence phase in the voter layer which perpetually drives the magnetization to zero. In this sense we name this phase as an active shattered phase, while in the shattered phase for $q = 1$ all isolated nodes are in the same state, which is the state in which the voter layer has reached a consensus. For large ℓ, S_1 increases and finally all nodes belong to one connected network component which is in a coexistence phase ($|m| = 0$). When ℓ is large, the voter layer which is in a dynamically active phase creates continuously active links in the dynamic layer as a consequence of the synchronization step of our dynamical model. Hence the fragmentation phase in the dynamic layer cannot be stable. In between these two phases, there is a critical value of the degree of multiplexity ℓ_c identifying a transition between an active shattered phase and a coexistence phase.

For the other type of nonlinearity $q > 1$, for example when $q = 2$, the shattered phase disappears ($nc \approx 0$) and S_1 gradually increases as ℓ increases (figures 6(c), (f)). Instead of the shattered phase, we find an asymmetric fragmented phase in which $S_1 \approx 1 - S_2$ for all ℓ except $\ell = 1$. When $\ell = 1$, we recover a consensus phase with $S_1 = 1$ and $S_2 = 0$. The magnetization $|m|$ also increases with increasing ℓ since the difference between S_1 and S_2 increases linearly. This phase with separated and asymmetric size of two extensive clusters is also not observed in a coevolution dynamics of the nonlinear voter model in a single layer.

A phase diagram with respect to ℓ and q is shown in figure 7(e). We find three different phases already described above: (I) asymmetric fragmented phase, (II) active shattered phase, and (III) coexistence phase. Examples of the multilayer network configuration for the different phases are also shown (figures 7(a)–(d)). When $q < 1$, we find a transition at ℓ_c between the active shattered and coexistence phases in the dynamic layer $L1$ while the voter layer $L2$ remains in a dynamically active coexistence phase (figure 7(c)). When $\ell \approx 1$, the dynamic layer $L1$ also maintains a large active coexistence component due to the high degree of multiplexity (figure 7(d)). When $q > 1$, the dynamic layer $L1$ exhibits two large connected clusters but with asymmetric sizes. In addition, the size difference of the two clusters decreases linearly with ℓ (figures 7(a), (b)). Phases (I) and (II) are not found in coevolution dynamics either in a single component network [36] or in a multilayer with linear

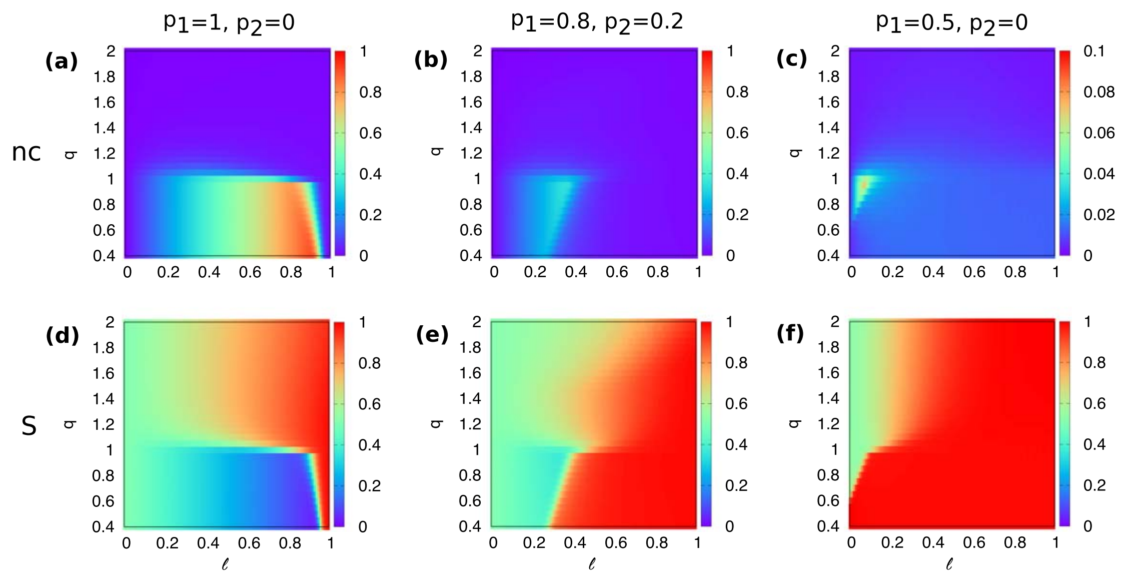

Figure 8. The relative number of components nc and size S of the largest component as a function of nonlinearity q and the degree of multiplexing ℓ for partially asymmetric plasticities (a), (d) $(p_1, p_2) = (1, 0)$ (b), (e) $(0.8, 0.2)$, and (c), (f) $(0.5, 0)$ on multilayer networks with $N = 10^3$.

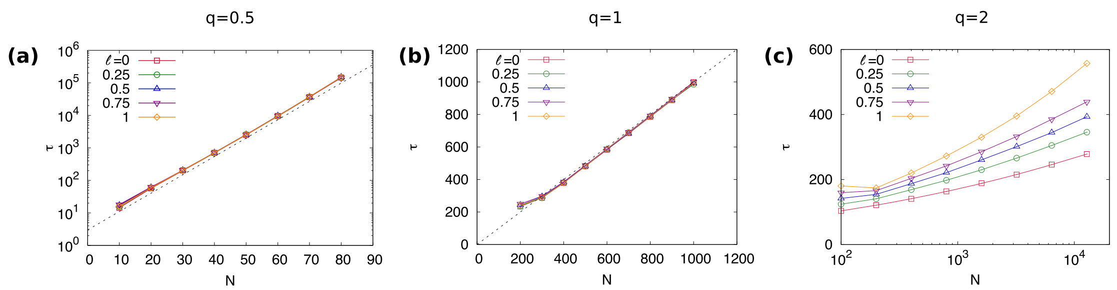

Figure 9. The characteristics time τ to reach steady state as a function of system size N for (a) $q = 0.5$, (b) $q = 1$, and (c) $q = 2$ for different ℓ and $(p_1, p_2) = (1, 0)$.

interactions [24]. Phase (III) is the analog of the dynamically active coexistence phase found in the single layer case, now with the same phase in the two layers. The difference is that in the present multilayer case this phase exists for $\ell > \ell_c$ as a consequence of large plasticity asymmetry, while in the single layer case it only exists below the fragmentation transition ($p < p_c$) as in the coexistence phase (b) in (figure 5)

The relative number of components nc and the size of the largest component S of the dynamic layer $L1$ as a function of q and ℓ is shown in figure 8 for the fully asymmetric case $p_1 = 1$ and $p_2 = 0$ and compared with results for partially asymmetric coupling ($p_1 \neq p_2$). For the partially asymmetric cases, i.e. $(p_1, p_2) = (0.8, 0.2)$ (figure 8(b)) and $(0.5, 0)$ (figure 8(c)), we find that the shattered phase where nc is nonzero is still present but in a smaller range of parameters than for the fully asymmetric case. This finding implies that asymmetric plasticity is the source of the shattered phase so that the area in the (q, ℓ) parameter space where shattering occurs is maximized at fully asymmetric coupling. In addition, a sharp transition at $q = 1$ indicates that the type of nonlinearity essentially determines the form of the fragmentation transition. For $q > 1$, the values obtained for S indicate that the asymmetric fragmentation phase also exists for general asymmetric values of the plasticity (figures 8(d)–(f)). The range of parameters in which this phase exists is maximized at the fully asymmetric coupling, while for small asymmetry in the plasticity values a consensus phase also exists. In summary, the new phases found for the fully asymmetric case continue to exist when the two layers have different plasticities.

Finally, we calculate the characteristic time τ to reach an absorbing state for different values of the nonlinear parameter q (figure 9). For $q = 0.5$, τ increases exponentially with the system size N, (figure 9(a)), so that in the thermodynamic limit ($N \to \infty$) we have a dynamically active coexistence phase and no absorbing state is reached. For finite systems, a finite size fluctuation will eventually take the system to an absorbing state, but due to the exponential dependence of the characteristic time on N, this is very rarely seen in our simulations and we observe dynamically active configurations which are extremely long lived. When $q = 1$, the characteristic time

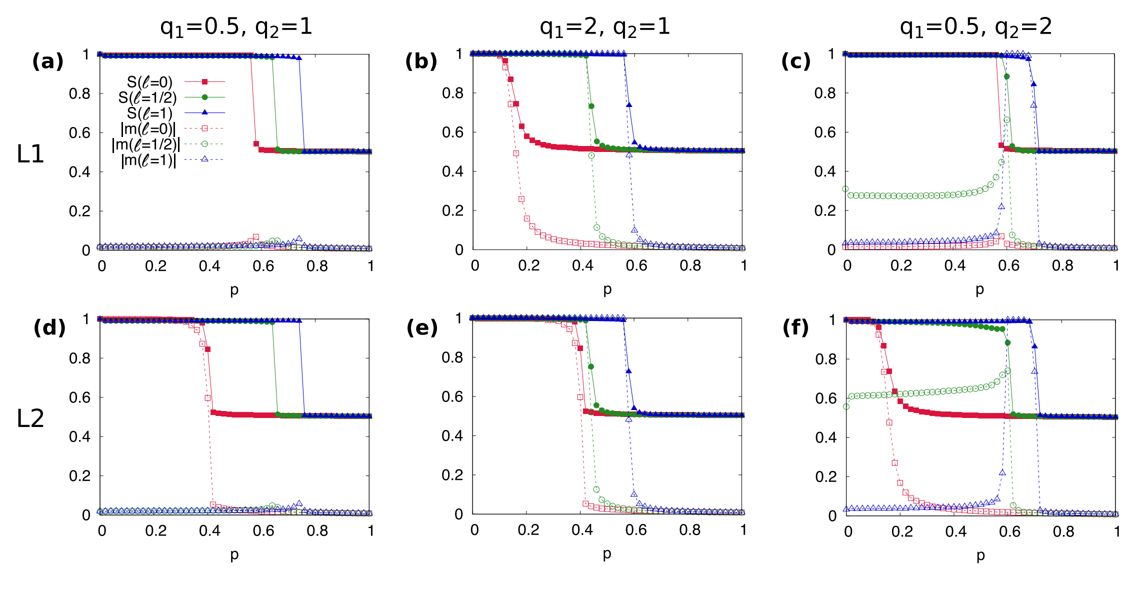

Figure 10. The size S of the largest component and the absolute value $|m|$ of magnetization of (a), (d) $(q_1, q_2) = (0.5, 1)$, (b), (e) $(2, 1)$, and (c), (f) $(0.5, 2)$ for different $\ell = 0, 0.5, 1$ on multilayer degree regular networks with $\langle k \rangle = 4$ and $N = 10^4$ for each layer.

grows linearly with the system size N, in the same way as in the usual voter model (figure 9(b)). In contrast, τ increases logarithmically with N for $q = 2$ (figure 9(c)), so that the absorbing state is reached in a relatively short time. The different scaling with N of these characteristic times, for different values of the nonlinear parameter q, is consistent with previous results for a CNVM on a single layer network [36] and also with local rewiring [37].

5. Asymmetric nonlinearity in multilayer networks

In this section, we consider the situation in which the two layers have a different nonlinear parameter q. Specifically, we consider three different cases $(q_1, q_2) = (0.5, 1), (2, 1), (0.5, 2)$ with the same plasticity parameter for both layers $p = p_1 = p_2$ (figure 10). For the cases $(q_1, q_2) = (0.5, 1)$ and $(q_1, q_2) = (2, 1)$, we find that the transition point p_c is shifted for both layers with increasing ℓ, in a similar way than we found for the symmetric nonlinearity case (see figure 2). In this case of asymmetric nonlinearity the layer that has slower dynamics (longer characteristics time τ) determines the steady state of the coevolving dynamics. For instance, when two layers with $q = 0.5$ and $q = 1$ are coupled, the layer with $q = 0.5$, with τ that grows exponentially with N, dominates the dynamics, and hence the system shows a fragmentation transition between a coexistence phase and a fragmented phase similarly to what happens when $q_1 = q_2 = 0.5$. In other words, in the long time limit, coevolution dynamics is shaped by the layer taking longer to reach its final state.

We also find an anomalous fragmentation transition when two layers with different q are coupled. When $(q_1, q_2) = (0.5, 2)$ and $\ell = 1$, there exist two subsequent transitions: one is the transition between a coexistence phase and a consensus phase and the other is between a consensus phase and a fragmented phase as shown in figure 10(c). For intermediate $\ell = 0.5$, the system exhibits an asymmetric active phase, that is active but $|m| \neq 0$. These results exemplify the rich variety in phase transitions that occur in multilayer structures with heterogeneous layer nonlinearities.

6. Discussion

We have studied a coevolving voter model on bilayer networks, focusing on the combined effect of nonlinear interactions, network plasticity and the degree of multiplexity. We observe a rich phase diagram with a number of new different phases and transitions. When the two layers have the same network plasticity and nonlinear parameter, we obtain a fragmentation transition similar to the one obtained in a single layer [36], but the transition is systematically shifted to larger values of the plasticity when increasing the degree of multiplexity. Therefore, multiplexing prevents fragmentation [24] also for a nonlinear voter model. When the two layers have different plasticities p but the same nonlinear parameter, we find new phases that do not exist in a CNVM in a single layer, namely an asymmetric fragmented phase and a dynamically active shattered phase. These phases are also not found in the multilayer version of the ordinary linear voter model. Finally, when coupling a nonlinear layer with a linear one ($q = 1$) we find that the layer with smaller nonlinearity, which is the one that would reach the final state in a longer time for $q_1 = q_2$, dominates the dynamics. In addition, when coupling layers with different types of nonlinearity $q_1 < 1$ and $q_2 > 1$ we observe an asymmetric active phase and also, for complete multiplexing $\ell = 1$, we observe two subsequent transitions when increasing the plasticity parameter: from a coexistence phase to a consensus phase, and from consensus to an absorbing fragmented phase.

Acknowledgments

We acknowledge financial support from Agencia Estatal de Investigacion (AEI, Spain) and Fondo Europeo de Desarrollo Regional under Project ESoTECoS Grant No. FIS2015-63628-C2-2-R (AEI/FEDER,UE) and from Agencia Estatal de Investigacion (AEI, Spain) through the Maria de Maeztu Program for Units of Excellence in R&D (MDM-2017-0711). This work was supported by the National Research Foundation of Korea (NRF) grant funded by the Korea government (MSIT) (No. 2018R1C1B5044202).

References

[1] Vidal M, Cusick M E and Barabási A L 2011 *Cell* **144** 986
[2] White J G, Southgat E, Thomson J N and Brenner S 1986 *Phil. Trans. R. Soc.* B **314** 1
[3] Borge-Holthoefer *et al* 2011 *PLoS One* **6** e23883
[4] Verbrugge 1979 *Soc. Forces* **57** 1286
[5] De Domenico M, Solé-Ribalta A, Gómez S and Arenas A 2014 *Proc. Natl Acad. Sci. USA* **111** 8351
[6] Little R G 2002 *J. Urban Technol.* **9** 109
[7] Rosato V, Issacharoff L, Tiriticco F, Meloni S, Porcellinis S and Setola R 2008 *J. Crit. Infrastruct.* **4** 63
[8] Min B, Yi S-D, Lee K-M and Goh K-I 2014 *Phys. Rev.* E **89** 042811
[9] Kivelä M, Arenas A, Barthelemy M, Gleeson J P, Moreno Y and Porter M A 2014 *J. Complex Netw.* **2** 203
[10] Leicht E A and D'Souza R M 2009 arXiv:0907.0894
[11] Buldyrev S V, Parshani R, Paul G, Stanley H E and Havlin S 2010 *Nature* **464** 1025
[12] Lee K-M, Min B and Goh K-I 2015 *Eur. Phys. J.* B **88** 48
[13] Boccaletti S, Bianconi G, Criado R, del Genio C I, Gómez-Gardeñes J, Romance M, Sendiña-Nadal I, Wang Z and Zanin M 2014 *Phys. Rep.* **544** 1
[14] Wang Z, Wang L, Szolnoki A and Perc M 2015 *Eur. Phys. J.* B **88** 124
[15] Diakonova M, Nicosia V, Latora V and San Miguel M 2016 *New J. Phys.* **18** 023010
[16] Son S-W, Grassberger P and Paczuski M 2011 *Phys. Rev. Lett.* **107** 195702
[17] Min B and Goh K-I 2014 *Phys. Rev.* E **89** 040802
[18] Gómez S, Díaz-Guilera A, Gómez-Gardeñes J, Pérez-Vicente C J, Moreno Y and Arenas A 2013 *Phys. Rev. Lett.* **81** 028701
[19] Min B, Gwak S-H, Lee N and Goh K-I 2016 *Sci. Rep.* **6** 21392
[20] Min B and Zheng M 2018 *PLoS One* **13** e0195539
[21] Vazquez F, Serrano M A and San Miguel M 2016 *Sci. Rep.* **6** 29342
[22] Czaplicka A, Toral R and San Miguel M 2016 *Phys. Rev.* E **94** 062301
[23] Brummitt C D, Lee K-M and Goh K-I 2012 *Phys. Rev.* E **85** 045102
[24] Diakonova M, San Miguel M and Eguíluz V M 2014 *Phys. Rev.* E **89** 062818
[25] Amato R, Kouvaris N, San Miguel M and Diaz-Guilera A 2017 *New J. Phys.* **19** 123019
[26] Artime O, Fernández-Gracia J, Ramasco José J and San Miguel M 2017 *Sci. Rep.* **7** 7166
[27] Klimek P, Diakonova M, Eguiluz V M, San Miguel M and Thurner S 2016 *New J. Phys.* **18** 083045
[28] Lugo H and San Miguel M 2015 *Sci. Rep.* **5** 7776
[29] Szolnoki A and Perc M 2013 *New J. Phys.* **15** 053010
[30] Wang Z, Wang L and Perc M 2014 *Phys. Rev.* E **89** 052813
[31] Battiston F, Nicosia V, Latora V and San Miguel M 2017 *Sci. Rep.* **7** 1809
[32] Perc M and Szolnoki A 2010 *Biosystems* **99** 109–25
[33] Zimmerman M G, Eguíluz V M and San Miguel M 2004 *Phys. Rev.* E **69** 065102
[34] Vazquez F, Eguíluz V M and San Miguel M 2008 *Phys. Rev. Lett.* **100** 108702
[35] Holme P and Newman M E J 2006 *Phys. Rev.* E **74** 056108
[36] Min B and San Miguel M 2017 *Sci. Rep.* **7** 12864
[37] Raducha T, Min B and San Miguel M 2018 *Europhys. Lett.* **124** 3001
[38] Castellano C, Muñoz M A and Pastor-Satorras R 2009 *Phys. Rev.* E **80** 041129
[39] Nyczka P, Sznajd-Weron K and Cislo J 2012 *Phys. Rev.* E **86** 011105
[40] Jedrzejewski A 2017 *Phys. Rev.* E **95** 012307
[41] Peralta A F, Carro A, San Miguel M and Toral R 2018 *Chaos* **28** 075516
[42] Nowak A, Szamrej J and Latané B 1990 *Psychol. Rev.* **97** 362
[43] Nettle D 1999 *Lingua* **108** 95
[44] Abrams D M and Strogatz S H 2003 *Nature* **424** 900
[45] Vazquez F, Castelló X and San Miguel M 2010 *J. Stat. Mech.* **04** P04007
[46] Castelló X, Loureiro-Porto L and San Miguel M 2013 *Int. J. Sociol. Lang.* **221** 21
[47] Jalan S and Pradhan P 2018 *Phys. Rev.* E **97** 042314
[48] Moretti P and Muñoz M A 2013 *Nat. Commun.* **4** 2521
[49] Raducha T and Gubiec T 2017 *Physica* A **471** 427